Supplementary Information

Charge Ordering and Low Temperature Lattice Distortion in the β′-(BEDT-TTF)$_2$CF$_3$CF$_2$SO$_3$ Dimer Mott Insulator

I. Olejniczak, R. Wesołowski, H.O. Jeschke, R. Valentí, B. Barszcz, and J.A. Schlueter

SI1 The β′-(BEDT-TTF)$_2$CF$_3$CF$_2$SO$_3$ crystal structure

β′-(BEDT-TTF)$_2$CF$_3$CF$_2$SO$_3$ crystallizes in the triclinic space group P-1. The structure is characterized by layers of partially oxidized BEDT-TTF molecules separated by anionic layers. There are two crystallographically nonequivalent BEDT-TTF molecules (hereafter designated as molecules A and B) per unit cell. As illustrated in Figure 1, layers of BEDT-TTF molecules of type A are located at z = 0, while those of type B are located at z = 0.5 (Figure S1).

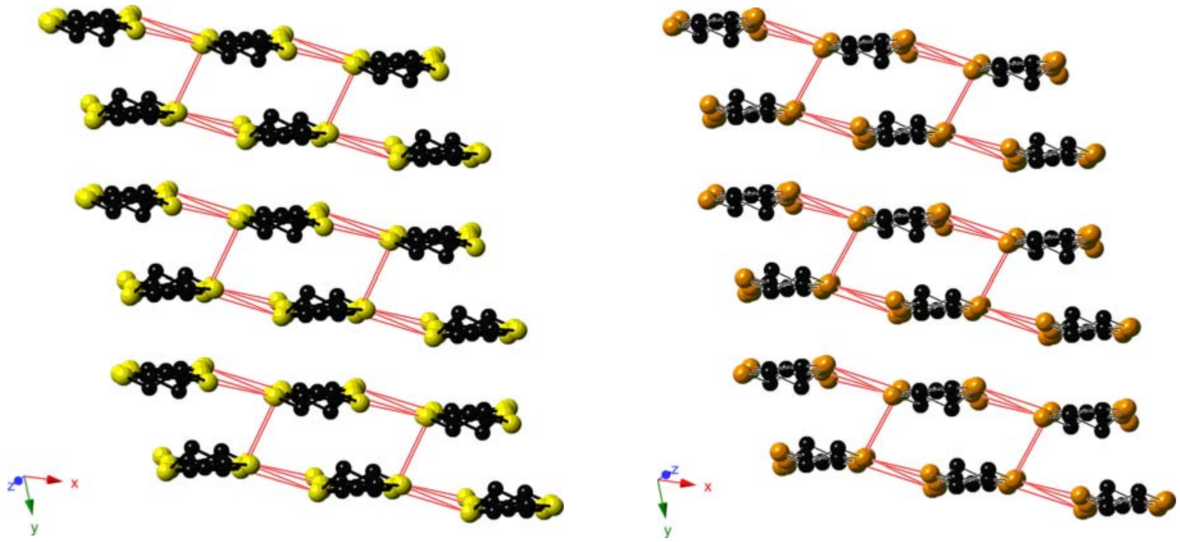

Figure S1. BEDT-TTF layers in β′-(BEDT-TTF)$_2$CF$_3$CF$_2$SO$_3$ at 100 K, located at z = 0 (left) and z = 0.5 (right), with hydrogen atoms removed for clarity; red lines indicate intermolecular S···S interactions shorter than 3.60 Å.

At room temperature the ethylene group associated with C17/C18 of molecule B is disordered (Figure S3), with 82% of the groups in the staggered conformation. At 100 K, there is no significant disorder in the cation layers with the ethylene groups of both molecules A and B (Figures S4, S5) in the staggered conformation.

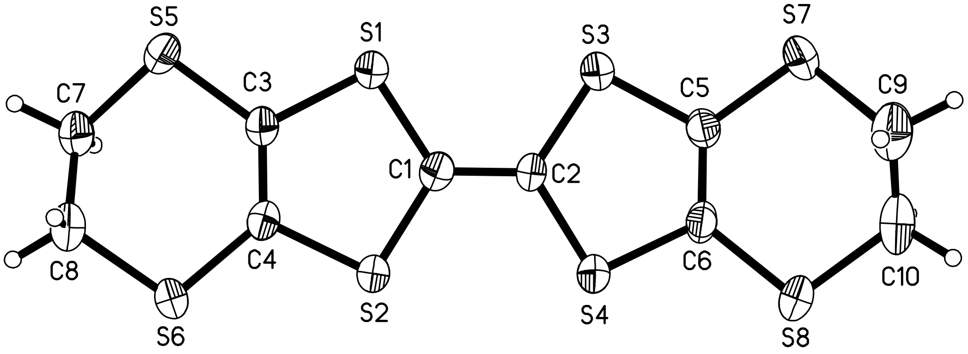

Figure S2. Thermal ellipsoid plot (50% probability level) with atom labeling scheme for the BEDT-TTF molecule (A) located at z = 0 in the β′-(BEDT-TTF)$_2$CF$_3$CF$_2$SO$_3$ structure at 300 K. Hydrogen atoms are drawn as spheres with arbitrary radius. Analysis of the bond lengths yields an oxidation state of +0.50.

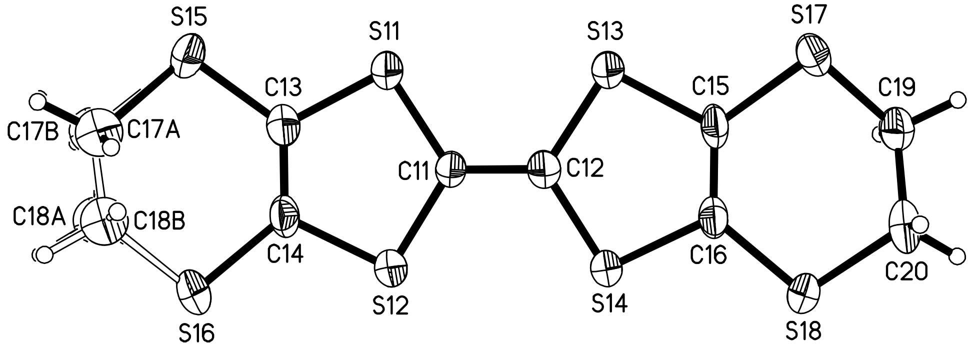

Figure S3. Thermal ellipsoid plot (50% probability level) with atom labeling scheme for the BEDT-TTF molecule (B) located at z = 0.5 in the β′-(BEDT-TTF)$_2$CF$_3$CF$_2$SO$_3$ structure at 300 K. The ethylene group associated with C17 and C18 is disordered with 82% occupancy in the staggered conformation with respect to C19/C20. Carbon atoms C17 and C18 are refined isotropically. Hydrogen atoms are drawn as spheres with arbitrary radius. Analysis of the bond lengths yields an oxidation state of +0.50.

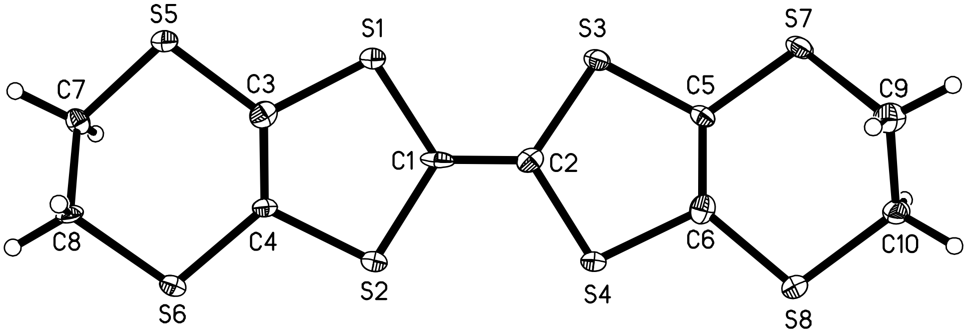

Figure S4. Thermal ellipsoid plot (50% probability level) with atom labeling scheme for the BEDT-TTF molecule (A) located at *z* = 0 in the β′-$(BEDT\text{-}TTF)_2CF_3CF_2SO_3$ structure at 100 K. Hydrogen atoms are drawn as spheres with arbitrary radius. Analysis of the bond lengths yields an oxidation state of +0.31.

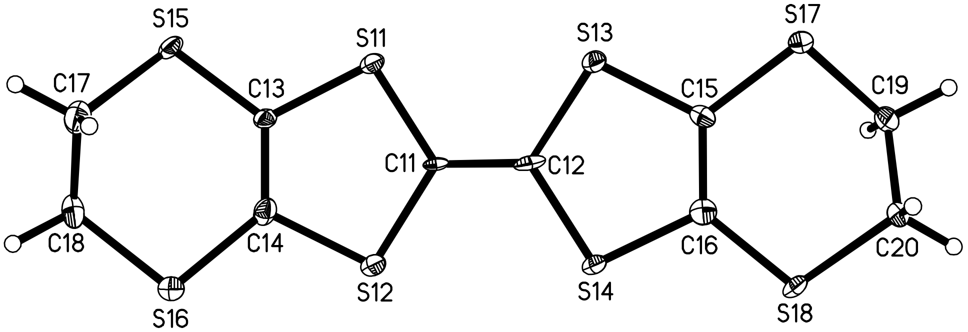

Figure S5. Thermal ellipsoid plot (50% probability level) with atom labeling scheme for the BEDT-TTF molecule (B) located at z = 0.5 in the β′-$(BEDT\text{-}TTF)_2CF_2CF_3SO_3$ structure at 100 K. Hydrogen atoms are drawn as spheres with arbitrary radius. Analysis of the bond lengths yields an oxidation state of +0.69.

A bond length analysis [1] indicates that at room temperature, the charges on all BEDT-TTF molecules are essentially identical. Assuming an integral -1 charge on the $CF_3CF_2SO_3^-$ anion, all BEDT-TTF molecules have a charge of +0.5. Upon cooling to 100 K, charge disproportionation appears to occur between the layers, with BEDT-TTF molecules A possessing a charge of +0.31 *e* and molecules B a charge of +0.69 *e*; here we define charge disproportionation (CD) as the difference in charge ρ between the charge-rich and charge-poor molecules. Due primarily to disorder within the anionic layer (see below), there is relatively large uncertainty (~0.15 *e*) in these bond-lengths. It has recently been pointed out that this method produces reliable results for perfectly refined structures (R1 < 0.05). However, with less well-refined structures, larger uncertainties can be expected due to the lighter carbon atoms being in close proximity to heavier sulfur atoms thus propagating error into the C=C bond length [2]. At room temperature

$CF_3CF_2SO_3^-$ anions are disordered over two configurations with 70% of the dominant orientation (see Figure S6). Upon cooling to 100 K, this disorder is not as well resolved (Figure S7) and was not successfully modeled in the crystal structure. Thus, the largest residual electron density was located 0.9 Å from the sulfur atom in the sulfonate anion. Inability to model this disorder led to a larger R value and greater uncertainty in the charge distribution obtained from a bond-length analysis.

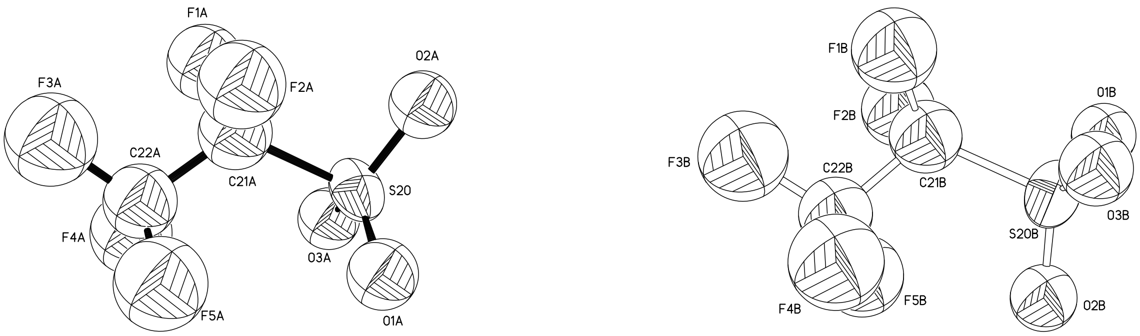

Figure S6. Two configurations of the disordered $CF_3CF_2SO_3^-$ anion in the β′-(BEDT-TTF)$_2$$CF_3CF_2SO_3$ structure at 300 K, including the atom labeling scheme. Thermal ellipsoids are drawn at the 50% probability level. 70% of the anions are in the primary (A) orientation.

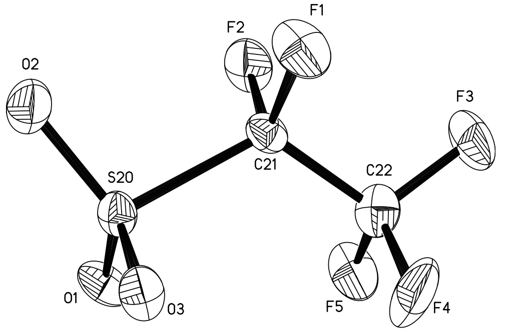

Figure S7. Thermal ellipsoid plot (50% probability level) with atom labeling scheme for the $CF_3CF_2SO_3^-$ anion in the β′-(BEDT-TTF)$_2$$CF_3CF_2SO_3$ structure at 100 K.

SI2 Other β′-phase structures of BEDT-TTF salts

From the point of view of structural properties, β′-(BEDT-TTF)$_2$$CF_3CF_2SO_3$ can be compared with the β′-(BEDT-TTF)$_2$$SF_5CF_2SO_3$ analog [3]. Although the BEDT-TTF radical cations in both the β′-(BEDT-TTF)$_2$$RCF_2SO_3$ (R = SF_5 or CF_3) structures pack in a β′-motif and have two crystallographically independent BEDT-TTF molecules, the overall structures are different. In the case of β′-(BEDT-TTF)$_2$$CF_3CF_2SO_3$, alternating layers have crystallographically unique molecules, while for β′-(BEDT-TTF)$_2$$SF_5CF_2SO_3$ (Figure S8) each layer is identical, but there are alternating stacks within the layers. This is likely a result of the difference in packing within the anion layers: in the case of β′-(BEDT-TTF)$_2$CF$_3$CF$_2$SO$_3$ the dipole moments of the CF$_3$CF$_2$SO$_3$ anions within a layer all point in the same direction, while in the case of β′-(BEDT-TTF)$_2$SF$_5$CF$_2$SO$_3$, the SF$_5$CF$_2$SO$_3$ dipoles point in opposing directions in adjacent chains within the layers.

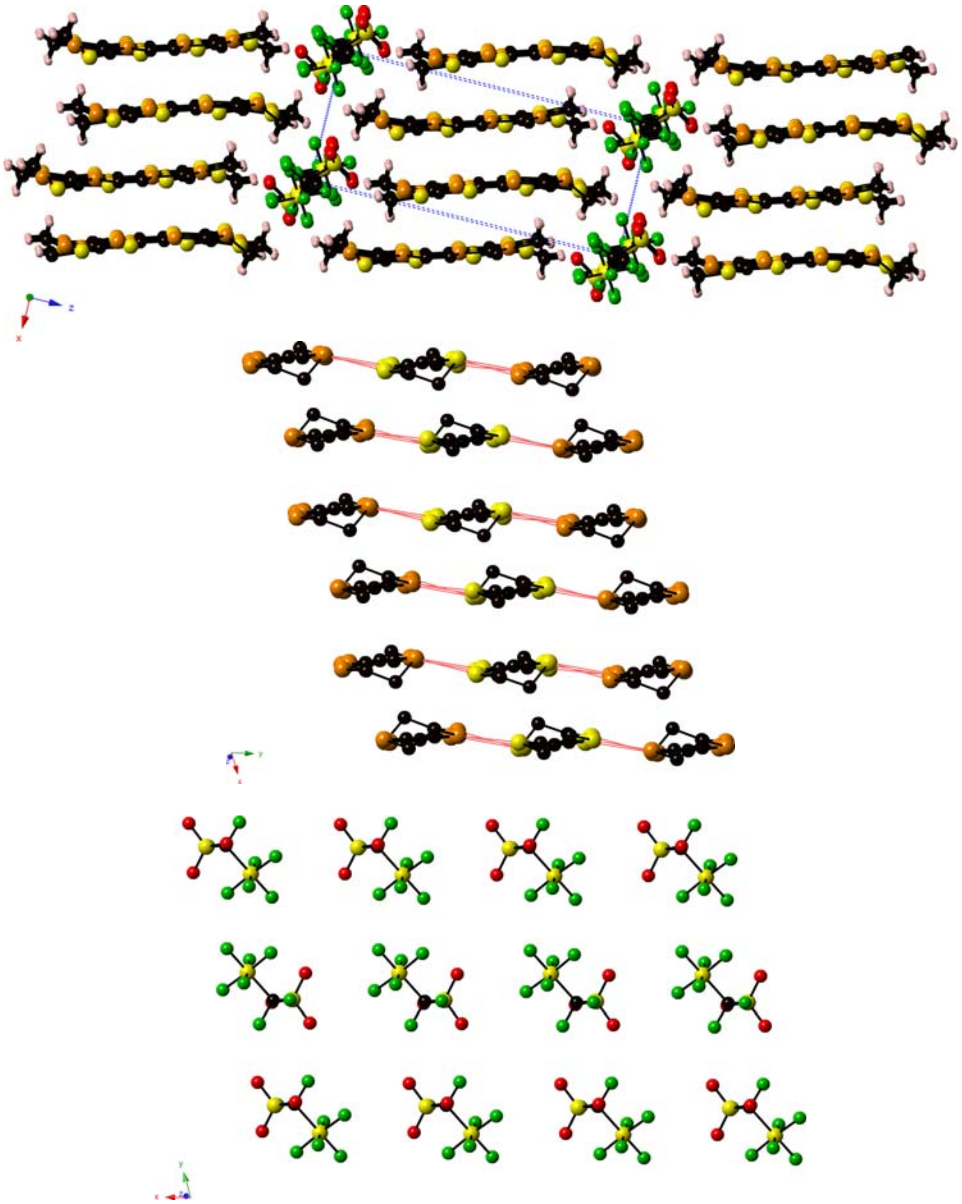

Figure S8. Packing diagrams of β'-(BEDT-TTF)$_2$SF$_5$CF$_2$SO$_3$ at 120K.

Similar effects have been seen in other BEDT-TTF salts. For example, in β′-(BEDT-TTF)$_2$ICl$_2$ there is a single crystallographically unique BEDT-TTF radical cation in the crystal structure (Figure S9), the anion is centrosymmetric and charge order is not expected in the BEDT-TTF layers [4]. Nevertheless, a recent dielectric study strongly suggests charge disproportionation within BEDT-TTF dimers in this compound [5].

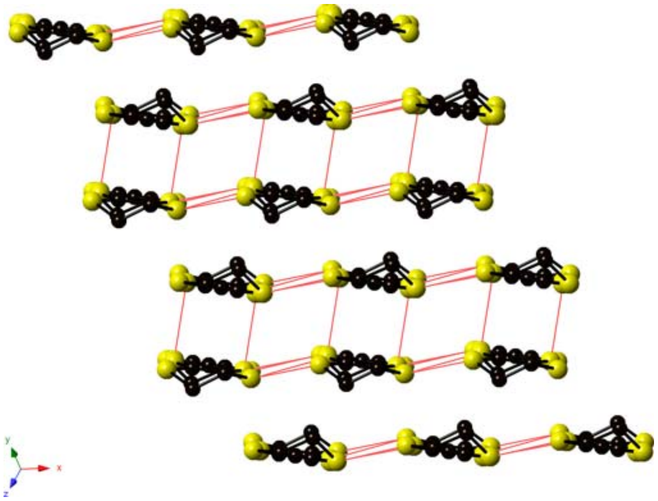

Figure S9. Packing diagram of β'-((BEDT-TTF)$_2$ICl$_2$ at T = 120 K.

SI3 Electronic bandstructure of β′-(BEDT-TTF)$_2$CF$_3$CF$_2$SO$_3$

In Figure S10 we show the calculated electronic band structures of T = 100 K and room temperature structures of β′-(BEDT-TTF)$_2$CF$_3$CF$_2$SO$_3$. The calculation is performed with two formula units in the $P\,\overline{1}$ unit cell. Thus, there are four bands arising from the highest occupied molecular orbitals of the BEDT-TTF molecules near the Fermi level. These four bands are approximately three-quarter filled. At this level DFT incorrectly gives a metallic system. Please note that inclusion of correlation effects beyond the PBE functional in terms of a many-body approximation such as dynamical mean field theory will describe the Mott insulating nature probed by the optical conductivity measurements. Such an approach has already been shown in the past to successfully describe the optical conductivity observations in other Mott insulating charge transfer salts [6].

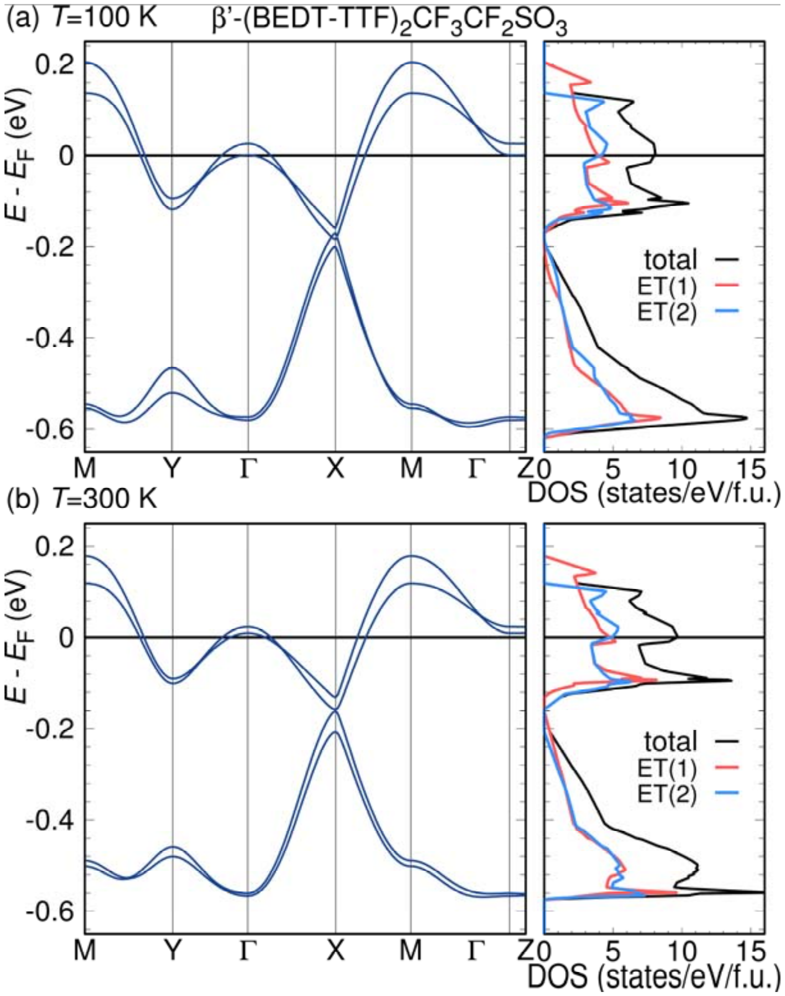

Figure S10. Bandstructures of β'-(BEDT-TTF)$_2$SF$_5$CF$_2$SO$_3$ at (a) T = 100 K and at (b) T = 300 K. ET stands for BEDT-TTF.

SI4 Lattice distortion observed in the infrared spectra of β′-(BEDT-TTF)$_2$CF$_3$CF$_2$SO$_3$

Optical conductivity spectra of β′-(BEDT-TTF)$_2$CF$_3$CF$_2$SO$_3$ suggest a significant lattice distortion takes place β′-(BEDT-TTF)$_2$CF$_3$CF$_2$SO$_3$ at about 25 K, most probably involving symmetry lowering. Unfortunately, no crystal data are available at low T to verify a possible symmetry lowering at the charge order transition as suggested by the Raman results. Nevertheless, the softening and intensity enhancement of several vibrational modes observed in the optical conductivity spectra (see the ν_3 mode components in Fig. S11) are consistent with a structural modification.

Other vibrational modifications are observed in the infrared spectra of β′-(BEDT-TTF)$_2$CF$_3$CF$_2$SO$_3$ along the **b-a** direction in the temperature range between 100 and 150 K. They can be related to ordering of the terminal ethylene groups that is characteristic for BEDT-TTF-based organic charge transfer salts [7,8]. We note a well-defined splitting the ν_5 mode involving symmetric bending of the BEDT-TTF ethylene groups that is centered between 1250 and 1300 cm^{-1} (Fig. S12). At the same time, another vibrational feature that appears at a frequency 1211 cm^{-1} below 150 K (Fig. S12) is identified as the SO_3 stretching mode of $CF_3CF_2SO_3$ anion (the ν_{SO3}). The temperature dependence of the selected ν_5 mode frequency (see the inset in Fig. S12) gives an estimate that is in line with the temperature scale of the ethylene groups ordering expected based on the crystal data. Therefore, the infrared spectra of β′-(BEDT-TTF)$_2$CF$_3$CF$_2$SO$_3$ provide an evidence that the anion layer is involved in the ethylene groups ordering in the donor layer below 150 K.

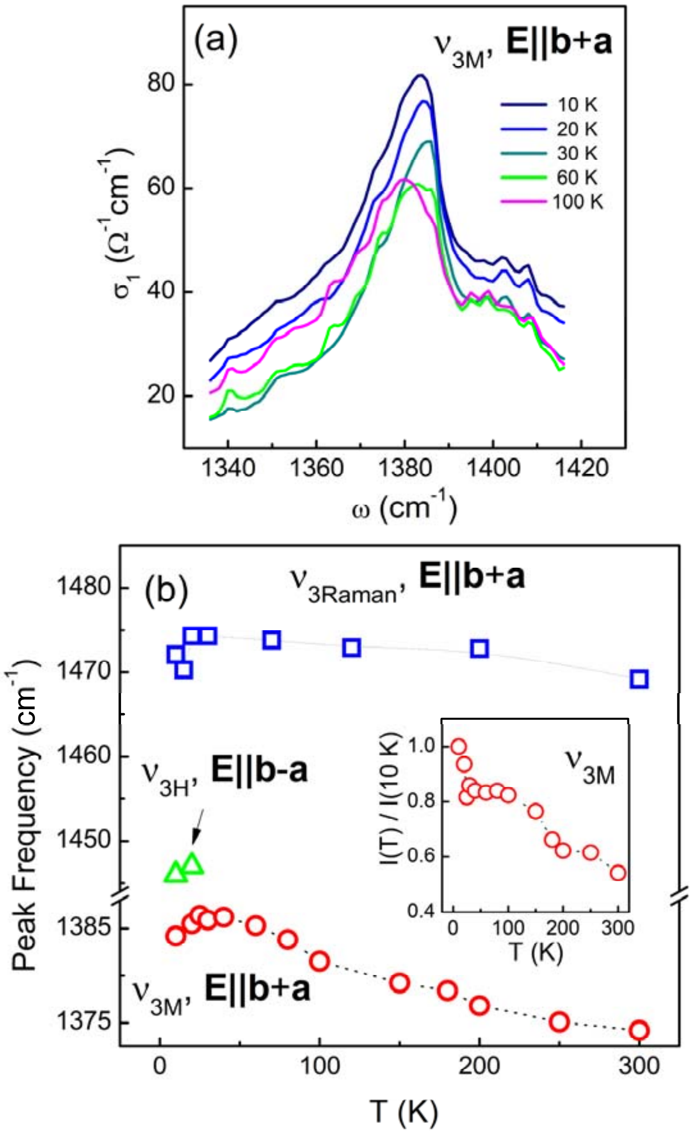

Figure S11. (a) Optical conductivity spectra of β′-(BEDT-TTF)$_2$CF$_3$CF$_2$SO$_3$ in the frequency range of the ν_{3M} vibrational BEDT-TTF mode at selected temperatures. (b) Temperature-dependent peak frequency of the ν_3 mode components: ν_{3M} and ν_{3S} observed in infrared spectra and ν_{3Raman} observed in Raman; inset: normalized intensity of ν_{3M}.

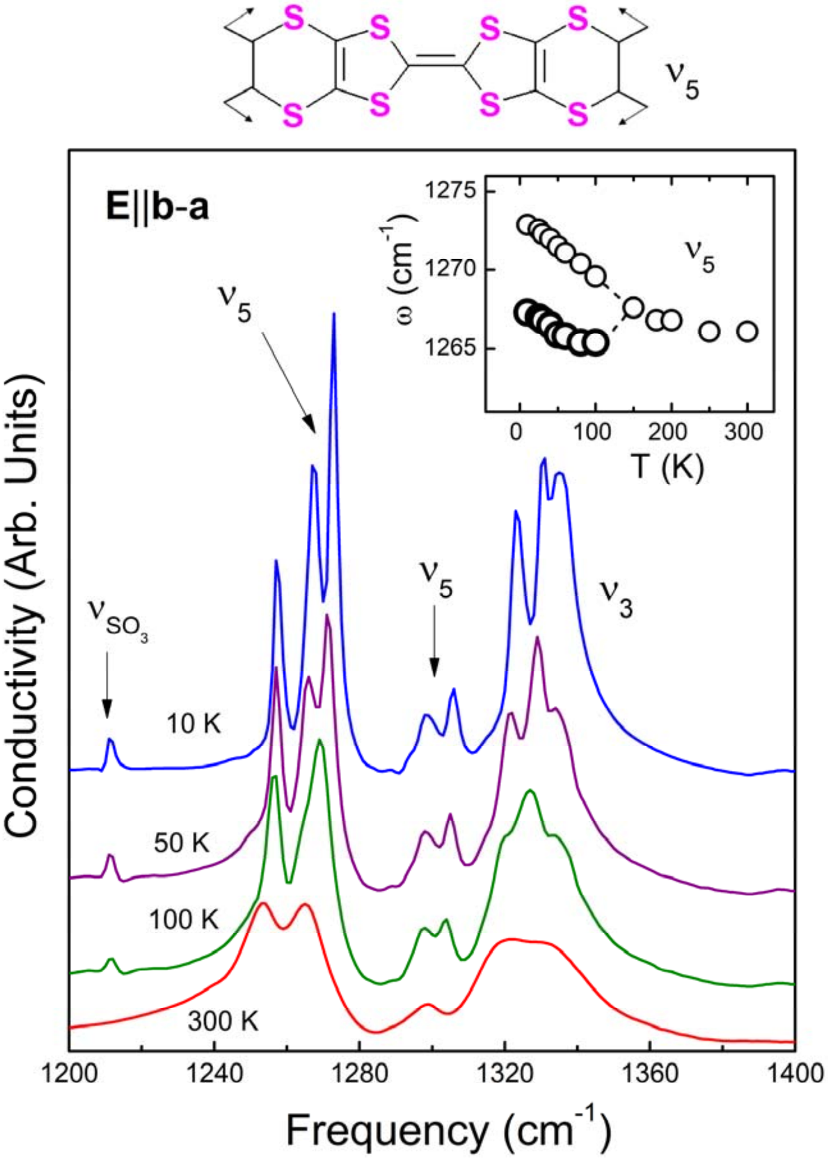

Figure S12. Temperature dependence of the electron-molecular vibration coupling-activated ν_3 stretching C=C mode and ν_5 wagging CH_2 mode of the BEDT-TTF donor molecule observed in optical conductivity spectra of β'-(BEDT-TTF)$_2$CF$_3$CF$_2$SO$_3$ in the **b-a** direction. Pronounced splitting of the ν_5 mode components is detected between 100 and 150 K, as shown in the inset. The smaller peak around 1200 cm^{-1} assigned to the stretching SO_3 mode of the $CF_3CF_2SO_3$ anion also appears in the spectra below 150 K. Spectra are shifted for clarity. Upper panel displays the ν_5 mode pattern.

References

1. P. Guionneau, C. J. Kepert, G. Bravic, D. Chasseau, M. R. Truter, M. Kurmoo, P. Day, Determining the charge distribution in BEDT-TTF salts, Synth. Met. **86**, 1973 (1997).

2. A. Bardin, unpublished work, 2015.

3. B. H. Ward, J. A. Schlueter, U. Geiser, H. H. Wang, E. Morales, J. P. Parakka, S. Y. Thomas, J. M. Williams, P. G. Nixon, R. W. Winter, G. L. Gard, H.-J. Koo, and M.-H. Whangbo, Comparison of the Crystal and Electronic Structures of Three 2:1 Salts of the Organic Donor Molecule BEDT-TTF with Pentafuorothiomethylsulfonate Anions $SF_5CH_2SO_3^-$, $SF_5CHFSO_3^-$, and $SF_5CF_2SO_3^-$, Chem. Mater. **12**, 343 (2000).

4. T. J. Emge, H. H. Wang, P. C. W. Leung, P. R. Rust, J. D. Cook, P. L. Jackson, K. D. Carlson, J. M. Williams, M.-H. Whangbo, E. L. Venturini, J. E. Schirber, L. J. Azevedo, and J. R. Ferraro, New Cation-Anion Interaction Motifs, Electronic Band Structure, and Electrical Behavior in β-$(ET)_2X$ Salts (X = $IC1_2^-$ and $BrICl^-$), J. Am. Chem. Soc. **108**, 695 (1986).

5. S. Iguchi, S. Sasaki, N. Yoneyama, H. Taniguchi, T. Nishizaki, and T. Sasaki, Relaxor ferroelectricity induced by electron correlations in a molecular dimer Mott insulator, Phys. Rev. B **87**, 075107 (2013).

6. J. Ferber, K. Foyevtsova, H. O. Jeschke, and R. Valentí, Unveiling the microscopic nature of correlated organic conductors: The case of κ-$(ET)_2Cu[N(CN)_2]Br_xCl_{1-x}$, Phys. Rev. B 89, 205106 (2014).

7. P. C. W. Leung, T. J. Emge, M. A. Beno, H. H. Wang, J. M. Williams, V. Petricek, P. Coppens, Novel structural modulation in the ambient-pressure sulfur-based organic superconductor β-$(BEDT\text{-}TTF)_2I_3$: origin and effects on its electrical conductivity, J. Am. Chem. Soc. **107**, 6184 (1985).

8. D. Guterding, R. Valentí, and H. O. Jeschke, Influence of molecular conformations on the electronic structure of organic charge transfer salts, Phys. Rev.B **92**, 081109(R) (2015), and references therein.